Infrared Counter-Countermeasure Efficient Techniques using Neural Network, Fuzzy System and Kalman Filter

M. R. Mosavi*

Abstract: This paper presents design and implementation of three new Infrared Counter-Countermeasure (IRCCM) efficient methods using Neural Network (NN), Fuzzy System (FS), and Kalman Filter (KF). The proposed algorithms estimate tracking error or correction signal when jamming occurs. An experimental test setup is designed and implemented for performance evaluation of the proposed methods. The methods validity is verified with experiments on IR seeker reticle based on a Digital Signal Processing (DSP) processor. The practical results emphasize that the proposed algorithms are highly effective and can reduce the jamming effects. The experimental results obtained strongly support the potential of the method using FS to eliminate the IRCM effect 83%.

Keywords: Fuzzy System, IRCCM, Jamming, Kalman Filter, Neural Network, Seeker.

1 Introduction

After the appearance of the first-generation Infrared (IR) seekers and their success against aircraft targets, a need for countermeasures against these seekers was emerged. A simple countermeasure against these seekers is an IR flare that can be deployed from the aircraft under attack. The flare intensity is usually several times that of the target radiation. The seekers bias their tracking points toward the more intense source. The seeker thus tracks a separating flare and loses track of the target. As the flare became a versatile and relatively effective Countermeasure (CM), seeker designers began to develop techniques to reduce offset the effectiveness of the flare [1].

The goal of active Infrared Countermeasures (IRCM) is add modulated IR energy to the IR signature of an aircraft to counter IR guided seekers. Aircraft power limitations, aircraft signatures, mission analysis, IR seeker signal processing, IR sources, and seeker-target simulation each play a critical role in the success of an active IRCM system [2].

Infrared Counter-Countermeasure (IRCCM) techniques against the IR flare may be based on the following differences between the target and the IR flare characteristics: temporal signal changes, spectral differences, trajectory differences (relative kinematics), and spatial size and distribution. Thus, a rapid increase in the seeker signal amplitude could be indicative of a flare deployment. However, signal fluctuations also could be caused by intentional or unintentional target radiation level changes [3].

The goal of this paper is to propose three new IRCCM efficient methods using Neural Network (NN), Fuzzy System (FS), and Kalman Filter (KF). These algorithms estimate tracking error or correction signal. The proposed methods validity is verified with experiments on IR digital seeker reticle based on a DSP processor. This paper is organized as follow. Section 2 describes jamming effects on seekers. The tracking error signal estimations based on NN, FS, and KF modeling are proposed in sections 3, 4, and 5, respectively. Experiments results are reported in section 6 and finally conclusions are presented in section 7.

2 Jamming Effects on Seeker

Typical modulation waveforms obtained for a constant radiation level target are shown in Fig. 1 [4]. The waveforms consist of an amplitude-modulated carrier. Signal processing removes the carrier and recovers the envelope of the waveform, which is at the reticle rotation frequency. The phase angle of this waveform relative to some reference determines the angular direction in which the seeker is driven to bring the target image to the center. Thus, a null point, where zero torque is applied, is obtained at the center of the reticle pattern since no modulation is generated there.

Iranian Journal of Electrical & Electronic Engineering, 2009.
Paper first received 18 Apr. 2009 and in revised form 16 Nov. 2009.
* The Author is with the Department of Electrical Engineering, Iran University of Science and Technology, Narmak, Tehran 16846, Iran.
E-mail: M_Mosavi@iust.ac.ir

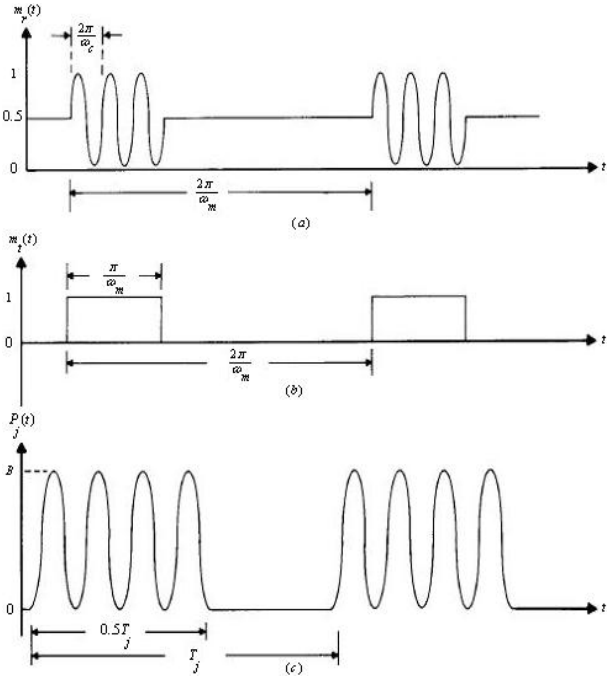

Fig. 1 Modulation waveforms: (a) typical modulation waveform, (b) carrier modulation function and (c) jammer modulation waveform

Consider a general case of a target with a collocated jammer that is modulated in time. The radiation power seen at the detector $P_d(t)$ may be represented by:

$$P_d(t) = [A + P_j(t)]m_r(t) \tag{1}$$

where, A is the target radiation power falling on the reticle, $P_j(t)$ is the time-modulated jammer power arriving at the reticle, and $m_r(t)$ is the reticle modulation function. The reticle modulation is periodic at the angular frequency of ω_m and can be represented by a Fourier series:

$$m_r(t) = \sum_{n=-\infty}^{\infty} c_n \exp(j\omega_m t) \tag{2}$$

where:

$$c_n = \frac{1}{T_m}\int_0^{T_m} m_r(t)\exp(-jn\omega_m t)dt \;;\; T_m = \frac{2\pi}{\omega_m} \tag{3}$$

If the jammer waveform is also periodic at the angular frequency of ω_j, $P_j(t)$ can be represented by:

$$P_j(t) = \sum_{k=-\infty}^{\infty} d_k \exp(j\omega_j t) \tag{4}$$

where:

$$d_k = \frac{1}{T_j}\int_0^{T_j} P_j(t)\exp(-jk\omega_j t)dt \;;\; T_j = \frac{2\pi}{\omega_j} \tag{5}$$

Substitution of Eq. (2) and Eq. (4) into Eq. (1) yields:

$$P_d(t) = [A + \sum_{k=-\infty}^{\infty} d_k \exp(j\omega_j t)]\times \sum_{n=-\infty}^{\infty} c_n \exp(j\omega_m t) \tag{6}$$

At the detector, $P_d(t)$ is converted into a voltage or current and is processed through a carrier amplifier, an envelope detector, and precession amplifier circuits before the signal is applied to drive the seeker. Consider the reticle modulation function is as shown in Fig. 1.a; i.e.,

$$m_r(t) = \frac{1}{2}[1 + \alpha m_t(t)\sin\omega_c t] \tag{7}$$

where, α is the ratio of the radius of the image location (or the tracking error) to the radius of the reticle that provides a simplified measure of the modulation efficiency $(0 \le \alpha \le 1)$, $m_t(t)$ is a carrier gating function (a square wave), as shown in Fig. 1.b, and ω_c is the carrier frequency. The Fourier series representation of $m_t(t)$ is:

$$m_r(t) = \frac{1}{2} + \frac{2}{\pi}\sum_{n=0}^{\infty}\frac{(-1)^n}{2n+1}\sin[(2n+1)\omega_m t] \tag{8}$$

Assume that the jammer modulation $P_j(t)$ also has the form of a carrier at the frequency ω_c and is gated at the frequency ω_j, as shown in Fig. 1.c; i.e.,

$$P_j(t) = \frac{B}{2}m_j(t)(1+\sin\omega_c t) \tag{9}$$

where, $m_j(t)$ has the same form as $m_t(t)$ except that ω_m is replaced by ω_j and B is the peak jammer power. The Fourier series representation for $m_j(t)$ is:

$$m_j(t) = \frac{1}{2} + \frac{2}{\pi}\sum_{k=0}^{\infty}\frac{(-1)^k}{2k+1}\sin\{(2k+1)[\omega_j t + \varphi_j(t)]\} \tag{10}$$

where, φ_j is an arbitrary phase angle relative to $m_t(t)$. For this special case Eq. (1) becomes:

$$P_d(t) = \frac{1}{2}[A + \frac{1}{2}Bm_j(t)(1+\sin\omega_c t)] \times [1 + \alpha m_t(t)\sin\omega_c t] \quad (11)$$

Assuming that the carrier amplifier passes signals at or near the carrier frequency only, the output of the carrier amplifier may be approximated by:

$$s_c(t) \approx \alpha[A + \frac{1}{2}Bm_j(t)]m_t(t)\sin\omega_c t + \frac{1}{2}Bm_j(t)\sin\omega_c t \quad (12)$$

The envelope of the carrier modulation in Eq. (12) is:

$$s_e(t) \approx \alpha A m_t(t) + \frac{B}{2}m_j(t)[1+\alpha m_t(t)] \quad (13)$$

The envelope signal $s_e(t)$ is further processed by a precession amplifier, which is tuned around the spin frequency ω_m. Assuming that ω_j is close to ω_m, the seeker driving signal is given by:

$$P(t) \approx \alpha(A + \frac{B}{4})\sin\omega_m t + \frac{B}{2}(1+\frac{\alpha}{2})\sin[\omega_j t + \varphi_j(t)] \quad (14)$$

The driving signal torques a spinning gyro (rotating magnet). The interaction of the rotating magnet and the seeker torquing signal results in the seeker precession rate proportional to the product of $P(t)$ and $\exp(j\omega_m t)$.

3 IRCCM Method using Neural Network

Multi-layer Perceptrons (MLPs) have been successfully used in time series prediction, however due to their multiple layer structure; they utilize computationally expensive training algorithms (such as the BP error) and can get stuck in local minima. In an attempt to overcome the problems associated with use of MLPs, High-Order NNs (HONNs) have been employed with great success. HONNs make use of nonlinear interactions between the inputs, thus functionally expanding the input space into another space, where linear separability, or reduction in the dimension of the nonlinearity is possible. However, HONNs suffer from the combinatorial explosion of the high-order terms and demonstrate slow learning, when the order of the network becomes excessively high. A simple yet efficient alternative to HONNs is the Pi-Sigma NNs (PSNNs). PSNNs are constructed of linear summing units with the output layer being a single product unit with a nonlinear transfer function. The weights from the summing units to the product units are fixed at unity, which implies that the summing units layer is not hidden. The degree of a PSNN equals the number of summing units in the first layer [5]. Fig. 2 shows a PSNN architecture.

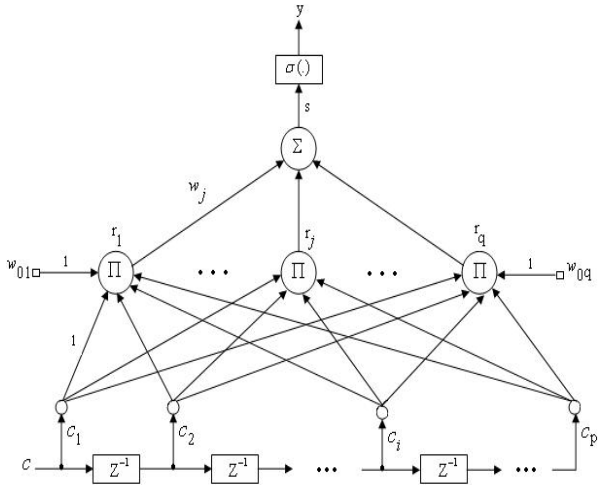

Fig. 2 Proposed PSNN with $(p,q,1)$ structure

The input c is a p dimensional vector and c_i is the $i-th$ component of c. The inputs are weighted and fed to a layer of q linear summing units, where q is the desired order of the neural network. w_{ji} is an adjustable weight from input c_i to the $j-th$ summing unit and w_{0j} is an adjustable threshold of the $j-th$ summing unit.

To achieve a desirable set of synaptic weights to a pre-defined network architecture, a training process in needed. A training process is generally based on an optimization scheme to adjust the network parameters (mainly, the weights) in relation to a set of input-to-output to be matched by the NN model (supervised learning scheme). The BP algorithm based on a gradient descent technique has been widely applied for general NN training. A BP employs a two-pass weighted learning algorithm known as the generalized delta rule. In a forward pass through the network, an error is detected; the measured error is then propagated backward through the network while weights are adjusted to reduce the overall error. This iterative process that the network goes through in reducing the overall error is known as gradient descent. The training steps are provided in the following subsection [6].

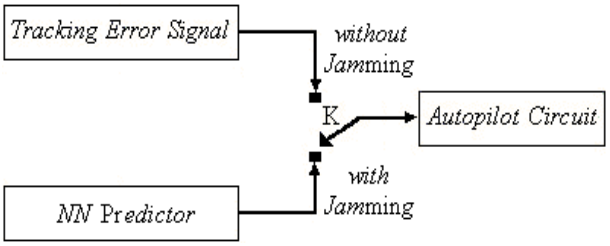

Fig. 3 Schematic diagram of proposed IRCCM method using NN

3.1 Training Steps

At first, some variables and parameters are defined:

$s_j =$ The output of the $j-th$ summing unit of hidden layer

$r =$ The net internal activity level of output neuron

$\sigma(.) =$ The activation function of output neuron as $\sigma(x) = 1/(1+e^{-x})$

$y =$ The output of the last output neuron

$\Delta w_{ji} =$ The adjusted value of the weight w_{ji}

$\Delta w_{0j} =$ The adjusted value of the threshold w_{0j}

$\eta =$ The learning-rate parameter

$\mu =$ The momentum value

Step 1: Weights Vector Initialization

Set all of the synaptic weights and threshold of the networks to small random numbers that are uniformly distributed.

Step 2: Forward Computation

$$s_j(m) = \sum_{i=1}^{i=p} w_{ji}(m)c_i(m) + w_{0j}(m)\ ;\ j = 1,2,\cdots,q \quad (15)$$

$$r(m) = \prod_{j=1}^{j=q} s_j(m) \quad (16)$$

$$y(m) = \delta[r(m)] = \delta\left(\prod_{j=1}^{j=q} s_j(m)\right) \quad (17)$$

Step 3: Learning Process

$$\Delta w_{0j}(m+1) = \eta(y(m) - d(m))y(m) \times (1 - y(m))\left(\prod_{l=1, l\neq j}^{l=q} s_l(m)\right) + \mu\Delta w_{0j}(m) \quad (18)$$

$$\Delta w_{ji}(m+1) = \eta(y(m) - d(m))y(m) \times (1 - y(m))\left(\prod_{l=1, l\neq j}^{l=q} s_l(m)\right)c_i(m) + \mu\Delta w_{ji}(m) \quad (19)$$

or:

$$\Delta w_{ji}(m+1) = (\Delta w_{0j}(m+1) - \mu\Delta w_{0j}(m)) \times c_i(m) + \mu\Delta w_{ji}(m) \quad (20)$$

Step 4: Iteration

Increment time m by one unit and go back to step 2.

Standard supervised BP learning methodology is followed in these experiments with PSNN. A subset of available actual data is used to construct training samples for the network. Training of a PSNN involves obtaining optimal values for the learning rate, the momentum of learning, and the number of nodes in each layer. The overall error is tracked until a minima is obtained by altering the fore-mentioned parameters. A trained network which has learned the sequential information in the training set can then be used in tracking error signal estimation. A 5-3-1 architecture with 5 inputs, one hidden layer of 3 nodes, and one output is used.

If the flare detection module declares the presence of a flare, the NN module estimates tracking error signal. The CCM tracking module will function until all flares exit the Field-of-View (FOV). After exit of all flares from FOV, the IRCCM method turns off CCM and returns to normal tracking. Fig. 3 shows schematic diagram of proposed IRCCM method using NN.

4 IRCCM Method using Fuzzy System

The generic seeker model consists of three modules: flare detection, CCM tracking, and normal tracking. The flare detection module attempts to determine whether flares exist within the FOV. If so, the CCM tracking module issues track commands in hopes of ignoring signals from flares. The normal tracking module issues track commands based on the weighted average of all sources within the seeker FOV [2].

There are three methods for flare detection. The first method computes the received intensity ratio for two different wavelength bands. It declares a flare if that ratio exceeds user-specified threshold. The next method tests the ratio of the instantaneous intensity to the historical average. If this ratio is above a user-defined threshold, it declares a flare. The final detection method monitors the seeker Line-of-Sight (LOS) rate. This method assumes the flare quickly separates from the aircraft thus causing a sudden change in the seeker LOS rate. This method declares a flare when the change in LOS rate exceeds a user-specified threshold.

Normally, the seeker electronics adjusts its gain to always keep the target source near the center of its dynamic range. If a flare is present and its intensity is much greater than that of the target, the seeker electronics can reduce its gain such that the signal from the target will fall below the noise floor of the electronics. Automatic Gain Control (AGC) locking stops this action. The flare intensity may cause the seeker electronics to saturate; however, the target intensity will remain within the seeker's dynamic range.

There are four track methods after flare declaration. The first method is rate hold. This technique adds an offset to the current tracking rate and holds that value. The next method is angle hold. This technique offsets and fixes the gimbal angles of the seeker. For these two methods, the offset causes the seeker to push ahead of the target. The hope is that the flare will exit the FOV and the target will move from the edge towards the center of the seeker FOV. The next method is rate bias. This technique uses the average of the previous tracking rate and the desired track rate for normal tracking. A user-defined value offsets this track rate in an attempt to

keep the seeker pointing ahead of the target. The final method is angle bias. This technique uses the desired gimbal angles for normal tracking and offsets it by a user-specified amount in the direction that the target was last moving. This attempts to keep the seeker pointing ahead of the target.

The block diagram of proposed IRCCM method using Fuzzy System (FS) is shown in Fig. 4. The $V_{o\,Error}$ is used as input fuzzy variable to this fuzzy system. Fuzzy system outputs are defined as $K1$ (a coefficient for $\varphi - angle$ signal) and $K2$ (a coefficient for tracking error signal). $\varphi - angle$ is angle between seeker axis and optical axis [7].

$V_{o\,Error}$, $K1$, and $K2$ are divided into two segments for partition the rule space. Those are fuzzied with a singleton membership function. The membership functions are defined as Fig. 5, where S and B express Small and Big, respectively.

Two rules in the rule base are defined as following:

$Rule1$: *If* $V_{o\,Error}$ *is Small,*

Then $K1$ *is* $S1$ *and* $K2$ *is* $B2$

$Rule2$: *If* $V_{o\,Error}$ *is Big,*

Then $K1$ *is* $B1$ *and* $K2$ *is* $S2$

The Mamdani-style method with product is used for the inference process and the center of area method is employed for the defuzzification [8]. If the flare detection module declares the presence of a flare, the FS module makes tracking error signal. The CCM tracking module will function until all flares exit the FOV. After exit of all flares from FOV, the IRCCM method turns off CCM and returns to normal tracking.

5 IRCCM Method using Kalman Filter

The Kalman Filter (KF) is a versatile procedure for combining noisy sensor outputs to estimate the state of a system with uncertain dynamics. This filter consists of three factors, which are prediction, observation, and estimation. The dynamic model describes the behavior of state vector, while the observation model establishes the relationship between measurements and the state vector. Both models are associated with statistical properties to describe the accuracy of the models.

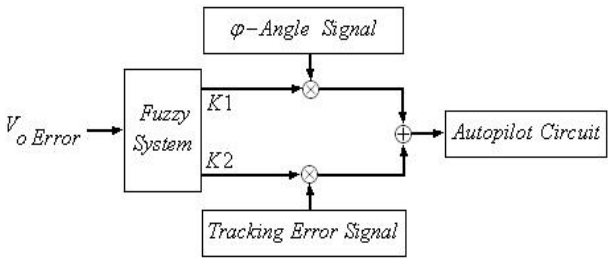

Fig. 4 Block diagram of proposed IRCCM method using FS

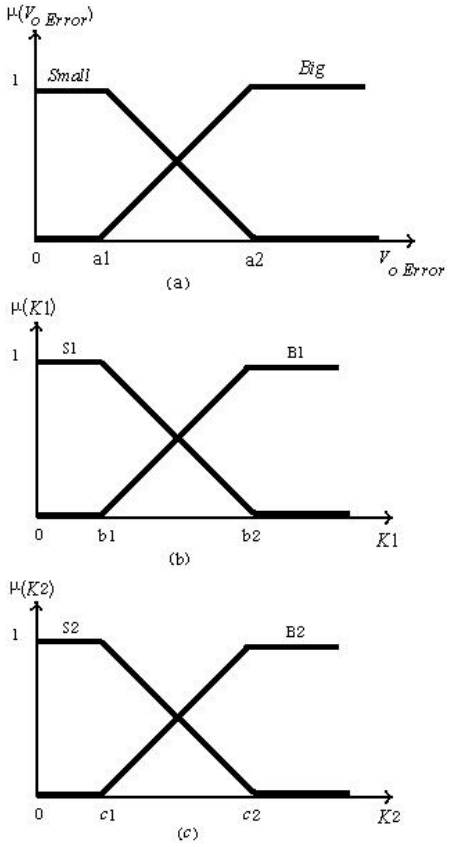

Fig. 5 Membership functions: (a) V_{oError}, (b) $K1$, and (c) $K2$

The KF is briefly described in this section. Assume that the random process is modeled in the form:

$$S[n+1] = A[n]S[n] + w[n] \quad (21)$$

where $S[n+1]$ is the process state vector at time $n+1$, $A[n]$ is a matrix relating $S[n]$ to $S[n+1]$ with the absence of a forcing function and $w[n]$ is white noise with known covariance structure. The measurement of the process is assumed to occur at distance points with the following relationship:

$$X[n] = H[n]S[n] + \gamma[n] \quad (22)$$

where $X[n]$ is the measurement vector at n, $H[n]$ is a matrix giving noiseless connection between the measurement and state vector at n and $\gamma[n]$ is the measurement error assumed to be white with a known covariance structure. The following KF equations for prediction are then derived as following [9]:

Step 1: Initial estimation for $\hat{S}[0]$ **and** $P^{-}[0]$

Step 2: Computation of Kalman gain

$$K[n] = P^{-}[n]H[n]^{T}(H[n]P^{-}[n]H^{T}[n] + R[n])^{-1} \quad (23)$$

Step 3: Updating the estimation with measurement $X[n]$

$$\hat{S}[n] = \hat{S}^{-}[n] + K[n](X[n] - H[n]\hat{S}^{-}[n]) \quad (24)$$

Step 4: Computation of error covariance for updated estimate

$$P[n] = (I - K[n]H[n])P^{-}[n] \quad (25)$$

Step 5: Updating the state transition matrix

$$A[n] = \begin{bmatrix} 0 & 1 & 0 \\ 0 & 0 & 1 \\ -a_{n1} & -a_{n2} & -a_{n3} \end{bmatrix} \quad (26)$$

where coefficients a_{n1}, a_{n2}, and a_{n3} are computed by fitting a three order time-varying Auto-Regressive (AR) model [10].

Step 6: Prediction

$$\hat{S}^{-}[n+1] = A[n]\hat{S}[n] \quad (27)$$

$$P^{-}[n+1] = A[n]P[n]A^{T}[n] + Q[n] \quad (28)$$

Step 7: Iteration

Increment time n by one unit and go back to step 2.

In Eq. (23) and Eq. (28), $R[n]$ and $Q[n]$ are obtained as:

$$E[w_k w_i^T] = \begin{cases} Q_k & ; \ i = k \\ 0 & ; \ i \neq k \end{cases} \quad (29)$$

$$E[v_k v_i^T] = \begin{cases} R_k & ; \ i = k \\ 0 & ; \ i \neq k \end{cases} \quad (30)$$

$$E[w_k v_i^T] = 0 \quad ; \quad \textit{for all } k \textit{ and } i \quad (31)$$

Equations (23)-(28) are used to perform Kalman filtering. A time series of N sample is provided. Then the coefficients of AR model are computed. AR is a well-known model used in discrete-time stochastic processes. The model update equations automatically provide one step prediction. The model updating continues for each prediction.

If the flare detection module declares the presence of a flare, the KF module estimates tracking error signal. The CCM tracking module will function until all flares exit the FOV. After exit of all flares from FOV, the IRCCM method turns off CCM and returns to normal tracking. Fig. 6 describes the proposed IRCCM method using KF.

6 Experimental Results

Performance of the proposed IRCCM methods was assessed with experiments on IR reticle seeker based on a DSP processor. Fig. 7 shows jamming detection system output. In this figure, Ch1 and Ch2 present information signal and jamming detection system output, respectively. As shown in Fig. 7, output of jamming detection system become from +15V to -15V, after jamming occurrence.

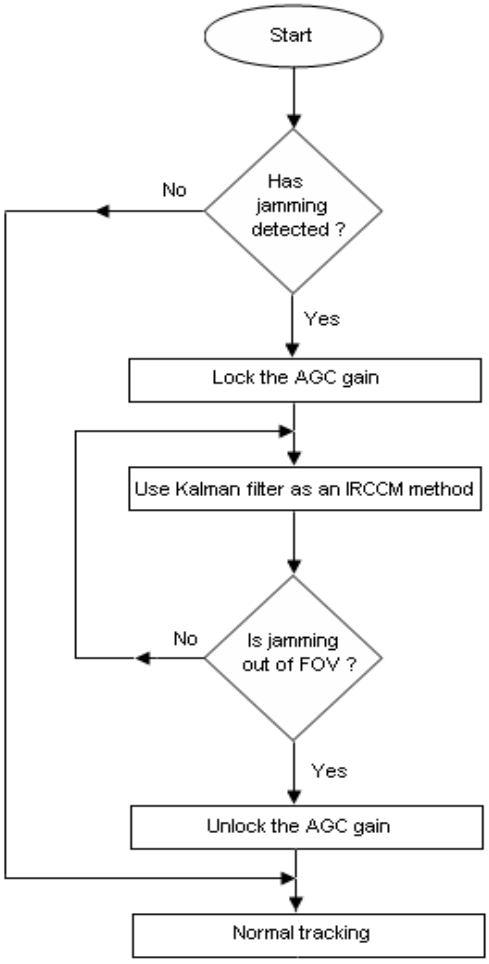

Fig. 6 Proposed IRCCM method description using KF

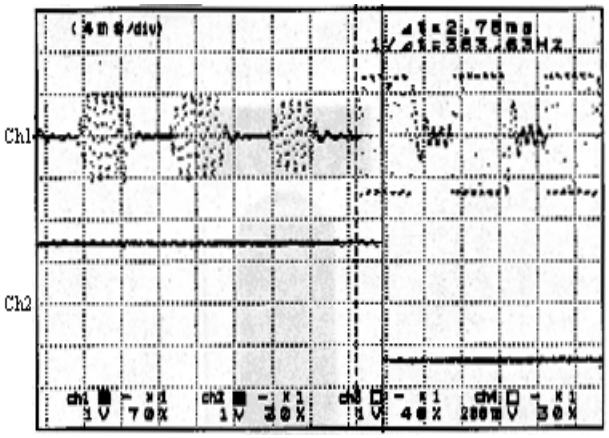

Fig. 7 Output of detection system, before and after jamming occurrence (Ch1: Information signal and Ch2: Detection system output).

Figs. 8, 9, and 10 show proposed IRCCM methods outputs using NN, FS, and KF, respectively. As shown in these figures, the proposed IRCCM methods can

properly estimate tracking error signal after jamming occurrence.

Fig. 11 shows a sample from running of developed IRCCM simulator program by paper author.

Table1 compares performance of the proposed IRCCM methods. As shown in this table, FS method is more accurate than other methods.

Table 1 Successful percentage results of proposed IRCCM methods

IRCCM Method	Present Algorithm	NN	KF	FS
Successful Percentage	39.6	54.5	62.5	83.3

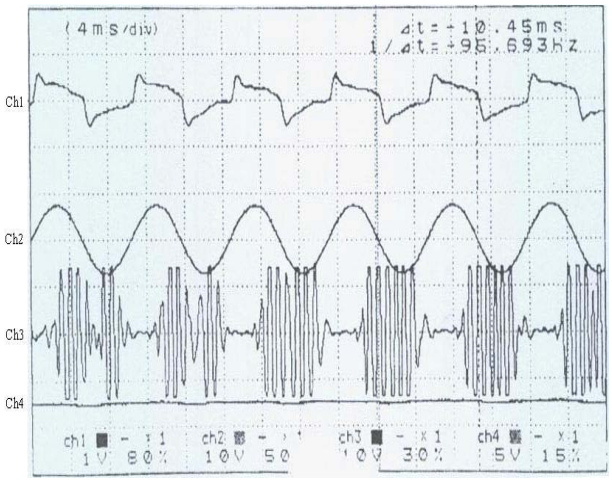

Fig. 8 Outputs of IRCCM method using NN (Ch1: NN output, Ch2: Tracking error signal, Ch3: Information signal, and Ch4: Detection system output).

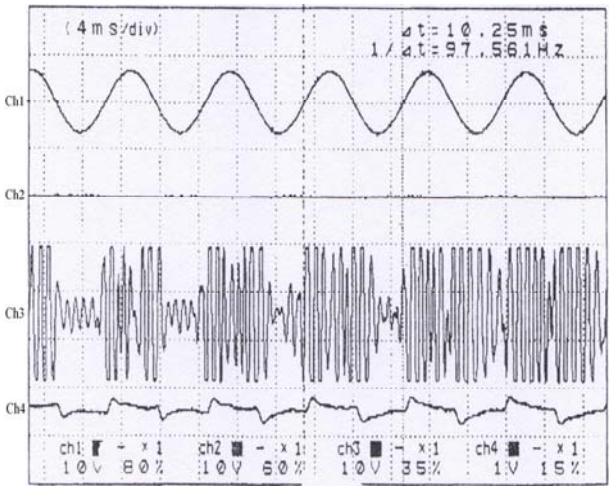

Fig. 9 Outputs of IRCCM method using FS (Ch1: Tracking error signal, Ch2: Detection system output, Ch3: Information signal, and Ch4: FS output)

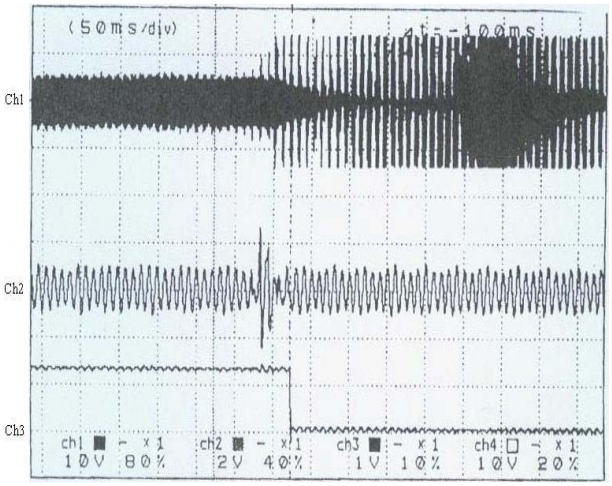

Fig. 10 Outputs of IRCCM method using KF (Ch1: Information signal, Ch2: KF output, and Ch3: Detection system output)

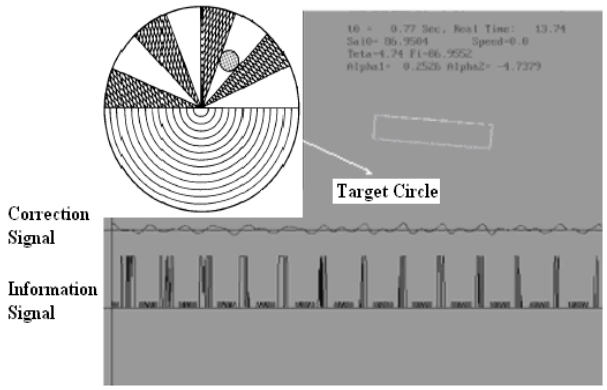

Fig. 11 A sample from running of developed IRCCM simulator program

7 Conclusions

In a target tracking system, an IRCCM algorithm is required for target efficient tracking under IRCM such as IR flares. The function of active IR jamming is to cause the seeker to miss its intended target by disturbing the seeker tracking process. The active IRCM acts in such a way as to cause either a complete loss of target tracking or to degrade target tracking in such a manner that the guidance of the seeker is affected adversely. This paper has presented design and implementation of three new IRCCM efficient methods using NN, FS, and KF. An experimental test setup was designed and implemented for performance evaluation of the proposed methods. The methods validity was verified with experiments on IR seeker reticle based on a DSP processor. The practical results emphasized that the proposed algorithms were highly effective and could reduce the jamming effects. The experimental results obtained strongly supported the potential of the method using FS to eliminate the IRCM effect 83%.

References

[1] Cohen R., Forrai D. and Maier J., "A Tool for Infrared Countermeasures Assessment," *IEEE Conference on Aerospace and Electronics*, pp.110-117, October 2000.

[2] Forrai D. P. and Maier J. J., "Generic Models in the Advanced IRCM Assessment Model," *Proceeding of the 2001 Winter Simulation Conference*, pp.789-796, 2001.

[3] Mosavi M. R., Asadpour M. and Kalili R., "Comparing Performance of Two Infrared Anti-Jamming Methods using Fuzzy System and Neural Network," *2007 Congress on Intelligent and Fuzzy Systems*, Ferdowsi University of Mashhad, Iran, August 2007.

[4] Mosavi M. R., Asadpour M., and Amerim H. A., "Design and Simulation of an Infrared Jammer Source for an Infrared Seeker," *IEEE Conference on Signal Processing, Communications, and Networking*, India, January 2008.

[5] Shin Y. and Ghosh J., "The Pi-Sigma Network: An Efficient High-Order Neural Network for Pattern Classification and Function Approximation," *IEEE Conference on Neural Networks*, pp.13-18, 1991.

[6] Mosavi M. R., "A Practical Approach for Accurate Positioning with L1 GPS Receivers using Neural Networks," *Journal of Intelligent and Fuzzy Systems*, Vol. 17, No. 2, pp.159-172, March 2006.

[7] Cui S. H. and Zhu C. Q., "Application of Kalman Filter to Bearing-Only Target Tracking System," *IEEE Conference on Signal Processing*, pp.1679-1682, 1996.

[8] Mosavi M. R., "Fuzzy Point Averaging of the GPS Position Components," *International Conference on Geographical Information Technology and Applications*, China, August 2004.

[9] Mosavi M. R., "Comparing DGPS Corrections Prediction using Neural Network, Fuzzy Neural Network, and Kalman Filter," *International Journal of GPS Solutions*, Vol. 10, No. 2, pp.97-107, May 2006.

[10] Mosavi M. R., Mohammadi K., and Refan M. H., "Time varying ARMA Processing on GPS Data to Improve Positioning Accuracy," *The Asian GPS Conference 2002*, pp.125-128, October 2002.

Mohammad-Reza Mosavi received his B.S., M.S., and Ph.D. degrees in Electronic Engineering from Iran University of Science and Technology (IUST), Tehran, Iran in 1997, 1998, and 2004, respectively. He is currently faculty member of IUST as associate professor. His research interests include Artificial Intelligent Systems, Global Positioning Systems, Geographic Information Systems and Remote Sensing.